# Optical observation of thermohydrodynamic flow in thin layers of superfluid $^4$He with a free surface

R. Meservey
*Francis Bitter National Magnet Laboratory, Massachusetts Institute of Technology, Cambridge, Massachusetts 02139*
(Received 14 November 1994)

An optical method of studying thermal counterflow in thin layers of superfluid $^4$He on a horizontal substrate is described. Solutions of the thermohydrodynamic equations give the slope of the liquid surface, the velocity fields, and the temperature gradients as a function of the heat current. The calculated surface slope as a function of heat current agrees with experimental observations below the critical heat current. Above the critical heat current there is evidence for a frictional force between the superfluid and the roughened substrate. At high heat currents turbulence and macroscopic vortices are observed and evidence for heat transfer through the vapor is found.

## INTRODUCTION

Recent optical experiments[1] on liquid $^3$He-*B* suggest that the description and analysis of earlier experiments with $^4$He may be useful. In addition, the development of laser, video, and optical fiber techniques makes the study of effects previously seen but not understood in $^4$He much more accessible. There have been a number of experiments[2,3] with superfluid $^4$He to observe the surface contour when a vessel containing the liquid is rotated and the optical observation technique used by Meservey[4] is similar to that described here for thermal counterflow.

Figure 1 shows schematically the general nature of thermal counterflow in a thin layer of superfluid $^4$He at low velocities. In these experiments a heater strip *H* forms normal fluid that flows toward the cold chamber wall resulting in the surface slope (greatly exaggerated in Fig. 1) caused by the viscosity of the normal fluid. The return flow of the superfluid is irrotational at low velocities. The thickness of the liquid layer $h$ is of the order of 0.1 mm. Over the heater there is a region of negative curvature determined by surface tension and then regions of uniform slope on each side of the heater which extend to within about 1 mm of the wall where surface tension dominates.

Above the $\lambda$ point the behavior is completely different. Over the heater strip is a depression of the liquid surface with positive curvature and just outside the heater a small region of negative curvature. Most of the liquid surface remains horizontal. The depression is caused by flow driven by a gradient in the surface tension which is the result of a temperature gradient, an effect explained by Hershey[5] (see also Landau and Lifshitz[6]). The effect is localized near the heater because the heat is carried to the wall by evaporative transfer. Below the $\lambda$ point, however, it is easy to show that this effect is very small compared with the effect of thermal counterflow and will be neglected.

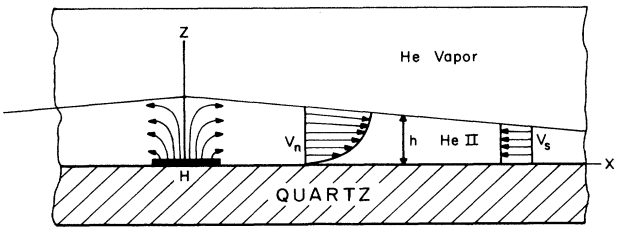


FIG. 1. Schematic diagram showing thermal counterflow in a thin layer of superfluid helium with a free surface.

## ANALYSIS OF THE LIQUID FLOW

The two fluid equations in regions with no source or sink of heat are assumed to be essentially those of Landau:[7]

$$\rho_s \frac{d\mathbf{V}_s}{dt} = -\frac{\rho_s}{\rho}\nabla\mathbf{p} + \rho_s S\nabla\mathbf{T} - \mathbf{F}_{SN} , \tag{1}$$

$$\rho_n \frac{d\mathbf{V}_N}{dt} = -\frac{\rho_n}{\rho}\nabla\mathbf{p} - \rho_s S\nabla\mathbf{T} + F_{SN} - \eta\nabla\times\nabla\times\mathbf{V}_N , \tag{2}$$

where $p$ is the pressure, $T$ the temperature, $S$ the entropy per unit mass, $\rho_n$ and $\eta$ are the density and viscosity of the normal fluid, $\rho_s$ the density of the superfluid, and $\rho_n+\rho_s=\rho$, the total density. The acceleration terms can be neglected outside the area of the heater. $F_{SN}$, the mutual friction force between the normal and superfluid, will be discussed below. In this case we obtain from Eqs. (1) and (2) expressions for the pressure and temperature gradients:

$$\nabla\mathbf{p} = -\eta\nabla\times\nabla\times\mathbf{V}_N , \tag{3}$$

$$\nabla\mathbf{T} = -\frac{1}{\rho S}\left[\eta\nabla\times\nabla\times\mathbf{V}_N - \frac{\rho}{\rho_s}\mathbf{F}_{SN}\right] . \tag{4}$$

We are concerned with a thin liquid layer of almost uniform thickness $h$ with a free surface and the velocities essentially limited to the $x$ and $y$ directions. In this case the pressure gradient can be expressed as

 

$$\nabla P = K\nabla T + \rho g \nabla h \ . \tag{5}$$

Here $K=(dP_V/dT)_T$ is the temperature dependence of the vapor pressure assumed to be a constant at a given working temperature $T$ because the temperature differences are extremely small. The second term is the gradient of the gravitational potential because of the small variations of the depth $h$. Equations (3)–(5) lead to equations for the surface slope and temperature gradient,

$$\nabla h = \frac{1}{\rho g}\left[-\eta(\nabla\times\nabla\times\mathbf{V}_N)(1-\alpha)-\alpha\frac{\rho}{\rho_s}\mathbf{F}_{SN}\right] , \tag{6}$$

$$\nabla T = \frac{1}{\rho S}\left[-\eta(\nabla\times\nabla\times\mathbf{V}_N)+\frac{\rho}{\rho_s}\mathbf{F}_{SN}\right] . \tag{7}$$

The inclusion of $\alpha=K/\rho S$ to account for the effect of vapor pressure at the free surface modifies these equations only slightly from those used in the analysis of counterflow in capillary tubes as, for instance, given by Childers and Tough.[8,9] $\alpha$ is the ratio of the vapor pressure to the thermomechanical pressure for a given temperature difference. The value of $\alpha$ is essentially independent of temperature in the range from 1.1 to 2.0 K and $1-\alpha\approx 0.925$.

With thermal counterflow in a thin layer originating in a line source, the velocities, to an excellent approximation, are limited to the $x$ direction and vary only in the vertical $z$ direction. Equations (4) and (5) then become

$$\frac{dh}{dx} = \frac{1}{\rho g}\left[\eta\frac{d^2V_N}{dz^2}(1-\alpha)-\alpha\frac{\rho}{\rho_s}F_{SN}\right] , \tag{8}$$

$$\frac{dT}{dx} = \frac{1}{\rho S}\left[\eta\frac{d^2V_N}{dz^2}+\frac{\rho}{\rho_s}F_{SN}\right] . \tag{9}$$

At low heat currents and therefore low velocities, $F_{SN}=0$ and Eq. (8) can be integrated with the boundary conditions

$$V_N=0 \quad at\ z=0 \text{ (at the substrate)} ,$$

$$dV_N/dz=0 \quad at\ z=h \text{ (at the liquid surface)} .$$

to give

$$V_N = \frac{dh}{dx}\frac{\rho g}{\eta(1-\alpha)}\left[\frac{z^2}{2}-hz\right] \tag{10}$$

and an average normal fluid velocity of

$$\bar{V}_N = -\frac{dh}{dx}\frac{\rho g h^2}{3\eta(1-\alpha)} . \tag{11}$$

$V_N$ can be expressed in terms of the heat current density $\dot{q}$

$$V_N = \dot{q}/\rho S T , \tag{12}$$

so that at low velocities where $F_{SN}=0$,

$$dh/dx = -3\eta(1-\alpha)\dot{q}/(h^2\rho^2 g S T) , \tag{13}$$

$$dT/dx = -3\eta\dot{q}/(h^2\rho^2 S^2 T) . \tag{14}$$

Above some critical heat current, previous experiments have shown that $F_{SN}\neq 0$ and we assume that

$$\mathbf{F}_{SN} = A\rho_s\rho_n|\mathbf{V}_S-\mathbf{V}_N|^2(\mathbf{V}_S-\mathbf{V}_N) , \tag{15}$$

the form originally proposed by Gorter and Mellink,[10] where $A$ varies only with $T$. Taking the curl of Eq. (1) with $dV_S/dt=0$ gives $\overline{\nabla\times\mathbf{V}_S}=\nabla\times\mathbf{V}_N$. In a limited region above the critical superfluid velocity, if we assume that the normal fluid flow is laminar and its velocity is still given by Eq. (10), then

$$\overline{dV_S/dz} = dV_N/dz . \tag{16}$$

The average sign over the curl of the superfluid is to emphasize that Eq. (16) actually means the equality of the circulation of the normal fluid and the superfluid over some macroscopic region containing many superfluid vortices. The assumption that the normal fluid flow remains laminar in a limited region above the critical heat current and that Eq. (16) holds in this region will be discussed below. The relative velocity $\mathbf{V}_S-\mathbf{V}_N$ is now independent of $z$ and conservation of mass, $\rho_s\bar{V}_S+\rho_N V_N=0$, gives

$$V_S-V_N = -\frac{\rho}{\rho_s}\bar{V}_N . \tag{17}$$

Since $F_{SN}$ is independent of $z$, Eqs. (8) and (9) can be integrated as before and together with Eq. (12) give

$$\frac{dh}{dx} = -\frac{1}{\rho g}\left[\frac{3\eta(1-\alpha)}{h^2\rho S T}\dot{q}+\frac{\alpha\rho_n\rho A}{(\rho_s S T)^3}\dot{q}^3\right] , \tag{18}$$

$$\frac{dT}{dx} = -\frac{1}{\rho S}\left[\frac{3\eta}{h^2\rho S T}\dot{q}+\frac{A\rho_n\rho}{(\rho_s S T)^3}\dot{q}^3\right] . \tag{19}$$

The assumptions made in deriving Eqs. (18) and (19) are that in region $B$, where the heat current density is somewhat above critical, the normal fluid flow remains laminar and that $F_{SN}$ has a form equivalent to Eq. (15). This picture, in which a first critical velocity corresponds to the entertainment of the superfluid vorticity to match the shear of the normal fluid and a higher critical velocity which marks a transition into isotropic turbulence, is hinted at by other experiments. In thermal counterflow, Tough and co-workers[11] have designated two distinct states of the dissipative superfluid, $T$I, which is definitely not homogeneous turbulence and $T$II, which approaches more closely the isotropic and homogeneous turbulence of the Schwartz theory.[12] Barenghi, Park, and Donnelly[13] find a vortex line density in thermal counterflow much less than that of homogeneous turbulence and a higher critical velocity corresponds to the transition to turbulence of the normal fluid. A similar picture emerges from experiments on rotating concentric cylinders, where it has been shown that in relatively high values of shear flow the superfluid vorticity approaches that of the normal fluid vorticity.[14] Again, at even higher velocities there is a second transition which corresponds to the

Reynolds number of normal fluid turbulence. These findings suggest that in region $B$ the vorticity of the superfluid may approximate that of the normal fluid and justify the derivation of Eqs. (18) and (19).

## APPARATUS

The apparatus is shown schematically in Fig. 2. Light from a Zr arc was collimated, passed through the movable aperture $A$, the beam splitter $B$, and down a thin-walled stainless steel tube, through four Vycor windows, which are tilted to avoid reflections along the optical axis and served to absorb thermal radiation. In addition, blackened baffles on the inside of the stainless-steel tube decreased the acceptance angle of room-temperature radiation. Light entered the experimental chamber $C$ and was reflected from the top surface of the thin layer of liquid helium $L$ and also from the quartz optical flat $Q$ which supported the He. The optical beams then returned to $B$ where they were directed through lens $D$ and observed or photographed in the image plane of $D$. The lower part of the stainless-steel tube and the experimental chamber were immersed in an outer bath of liquid helium that could be pumped on to reduce the temperature to 1.1 K. In the experimental chamber, a liquid level of the desired thickness (of the order of a fraction of a millimeter) was obtained by condensing a known quantity of He gas into $C$ from a storage volume $V$.

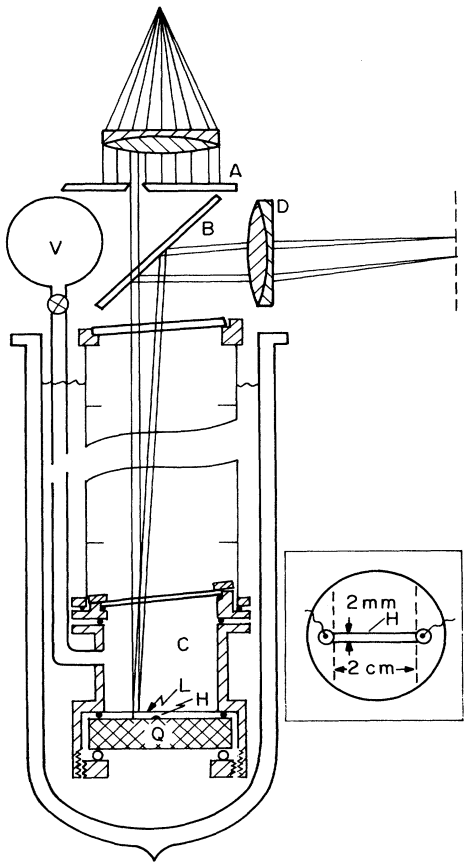


FIG. 2. Representation of the optical method of measuring the slope of the liquid He surface. The plan view inset shows the heater $H$. In the general view the heater line is perpendicular to the plane of the paper.

To measure the slope of the liquid surface, the movable aperture $A$ defined a narrow pencil of light to a particular position on the surface of the liquid $L$. The lens $D$ brought the pencil of light from the He surface to a point image in the focal plane of the lens $D$. A filar eyepiece allowed the position of the point image from the liquid surface to be measured with respect to the position of the point image formed by the reflection from the optical flat. From this measurement and the focal length of $D$, the angle of the surface of the liquid was obtained as a function of position as the aperture was moved.

To observe interference fringes between the optical flat and the liquid surface, the aperture $A$ was removed and the fringes were observed in the plane of the conjugate focus of the lens $D$ for the liquid helium surface. The reflectivity of the quartz optical flat was about 0.04, whereas that of liquid He was about 0.002. To obtain high contrast interference fringes, it was necessary to decrease the specular reflection from the optical flat that returned in the collimated beam, so that the amplitude of the reflection from the liquid and the substrate would be approximately equal. This was accomplished by lightly grinding the surface of the flat with No. 400 Alundum until only a small fraction of the area of the originally polished surface of the flat remained and this in small isolated spots. Thus the reflection from the flat remaining in the collimated beam was attenuated by a factor of about 200, and uniformity over the field of view is assured by diffraction from the remaining very small specularly reflecting areas. Fringes were visible for liquid depths less than 0.2 mm, provided there were no surface vibrations. With laser illumination, this depth limit for fringe observation would be removed.

The equipment was mounted on low-frequency antivibration supports and vacuum pumping lines were made of flexible tubing with a ballast to dampen vibrations from the vacuum pump used to lower the helium temperature.

## MEASUREMENTS AND OBSERVATIONS

Figure 3 shows the measured surface slope $dh/dx$ as a function of the heater power $\dot{Q}$ at 1.47 K. At low values of $\dot{Q}$ (region $A$ in Fig. 3) the surface slope increased linearly with heater power as predicted by Eq. (9). The power dissipated in the heat strip is

$$\dot{Q}=2\dot{q}/hW\ , \tag{20}$$

where $\dot{q}$ is the heat current density, $h$ the liquid depth, $W$ the length of the heater strip, and the factor of 2 accounts for the heat flow in both the $-x$ and $+x$ directions.

With low values of heat current, the liquid surface was roof shaped with a small area of negative curvature immediately above the heater strip. Beyond the heater the

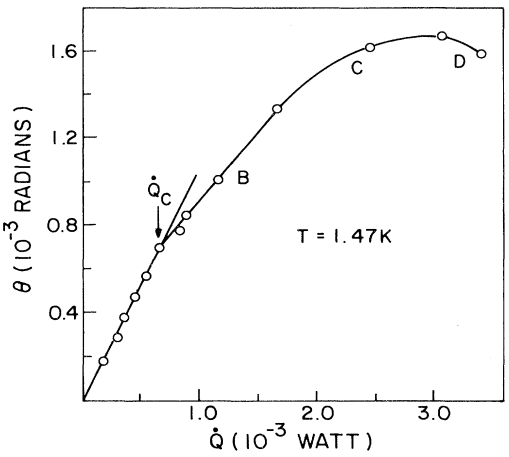


FIG. 3. Angle of the He surface versus input power at 1.47 K and liquid depth $h_e = 1.61 \times 10^{-2}$ cm.

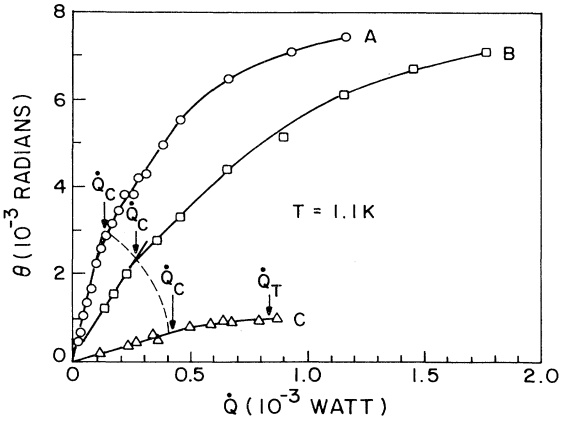


FIG. 5. Angle of the surface versus input power at 1.1 K and $h_e = 1.04 \times 10^{-2}$, $1.32 \times 10^{-2}$, and $2.58 \times 10^{-2}$ cm for curves *a*, *b*, and *c*, respectively.

surface slope was uniform within 5 or 10 percent for about 1 cm on each side of the heater for moderate heat currents. Most of the optical measurements of the surface slope were made with a 2 mm wide slit near the middle of the 1 cm range. An angular change of $10^{-5}$ rad could be detected, which is close to the diffraction limit.

At some critical value $\dot{Q}_c$ there was a sudden decrease in the rate of change of $|dh/dx|$ with $\dot{Q}$ and then another linear region *B*. At some not very well defined point, a negative curvature developed (region C), which lasted until $|dh/dx|$ started to decrease. Somewhere in region C, macroscopic turbulent flow would start to be observed as shown by the presence of irregularly spaced surface dimples (about 1 mm in diameter and several microns deep) moving in the direction of the heat current and caused by macroscopic vortex motion. The image of the focused light beam broadened in this region and disappeared as macroscopic turbulence developed. The behavior in the turbulent region could be observed by the shadowgraph effect caused by curvatures in the liquid surface focusing the parallel light beam. In region *D* there was extreme turbulence, a decrease of slope with power, and finally no specularly reflected image. Figure 4 shows an equivalent measurement of $dh/dx$ at 1.24 K and Fig. 5 shows measurements at 1.1 K and three different depths. All of the measurements at seven different temperatures were qualitatively like those of Fig. 3, except that the reflected image often disappeared before reaching region *D*.

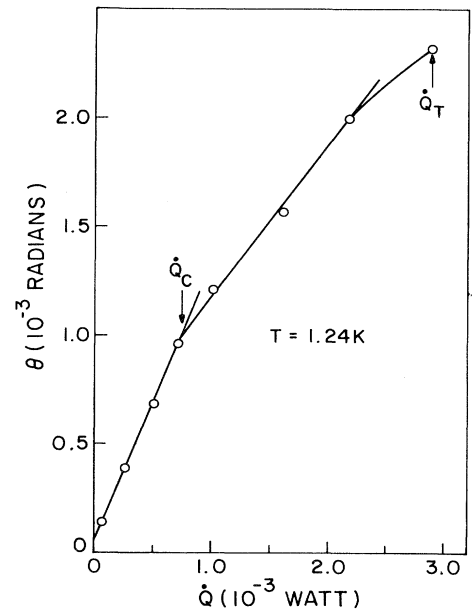


FIG. 4. Angle of the He surface versus input power at 1.24 K and liquid depth $h_e = 1.57 \times 10^{-2}$ cm.

### Results at low velocity

In quantitatively comparing Eq. (13) with the measured values of surface slope in region *A*, the greatest uncertainty was the thickness of the liquid layer *h*, which was determined in three ways. First, a known volume of gas was condensed into the system and the depth calculated from the pressures, temperatures, and volumes, and corrected for surface tension effects at the chamber walls. Unfortunately, the correction for the volume of liquid in the meniscus at the walls of the chamber was large, and led to making this value of the depth *h* unreliable. Second, the method usually used to obtain the liquid depth was to allow the temperature to rise until the liquid evaporated and the specular reflection from the liquid surface just disappeared. From the temperature at which this occurred and the volume and pressure of the gas, the liquid thickness $h_e$ was calculated and the surface tension correction was avoided. The third method of counting interference fringes as the liquid layer evaporated or condensed was much more accurate, but it was usually im-

TABLE I. Comparison of $h_\theta$, the liquid depth calculated from the plots of $\theta$ vs $\dot{Q}$ using Eqs. (13) and (20), and $h_e$, the depth determined from the evaporation temperature.

| $T$ (K) | $h_e$ ($10^{-2}$ cm) | $h_\theta$ ($10^{-2}$ cm) |
|---|---|---|
| 1.12 | 1.04 | 1.03 |
| 1.1 | 1.32 | 1.51 |
| 1.10 | 2.58 | 2.56 |
| 1.24 | 1.57 | 1.84 |
| 1.47 | 1.61 | 1.23 |
| 1.73 | 0.40 | 0.46 |
| 1.99 | | 0.66 |

practical to count the 200 to 1000 fringes because of the disappearance of fringes at unpredictable times caused by surface ripples.

To compare the results with the theory, we used the measurements of the slope of the liquid surface and the known liquid properties to calculate the liquid depth from Eq. (13) and have compared this depth $h_\theta$ with the depth $h_e$. This comparison is shown in Table I. The results show a fair correlation between the values of $h$. The important parameter $3\eta/2\rho^2 gSTL$ varies by a factor of more than 100 over these measurements and the average disagreement is 12%. The measurements at 1.12 K were able to use a depth determined by fringe counting and the values of $h$ agreed within 1%. It is concluded that the results at low heater power (region $A$) are consistent with Eq. (13).

### Results at higher velocities

The transitions from region $A$ to region $B$ are found at heat current densities and fluid velocities which correspond approximately to other measurements of the first critical velocity observed in channels of the same smallest lateral dimension.[8,9] In region $B$, the absolute value of the (negative) surface slope increases less rapidly than in region $A$, but still varies linearly with $\dot{Q}$.

The behavior in region $B$ cannot be explained by the second term in Eq. (18), which predicts a highly nonlinear *increase* in the absolute value of the surface slope above the critical velocity. Also, thermal counterflow experiments in tubes[8,9] have found a greater *increase* in the pressure gradient with heat current in the region above the critical heat current and so it does not correspond with the present results. A possible explanation of the smaller increase of surface slope above the critical heat current is that the rapid rise in the temperature gradient will lead to increased evaporative heat transfer through the vapor and therefore a decrease in the fraction of $\dot{Q}$ carried by the normal fluid. This effect would lead to a smaller rate of change of the surface slope and is close to the required magnitude at the lower temperatures. Unfortunately, no temperature measurements were made to check this conjecture accurately, but it seems probable that this mechanism is at least responsible for the nonlinear response in regions $C$ and $D$ and the eventual decrease in the absolute value of the surface slope in region $D$, as seen in Fig. 3.

A difference between thermal counterflow in tubes and the present experiments besides the free surface is that the substrate in the present experiments was very rough and the walls of the tubes used in thermal counterflow in tubes have been comparatively smooth. This fact might account for the present results. The eddy viscosity of the superfluid documented by Childers and Tough[8,9] may interact with the substrate as well as with the normal fluid. Such an interaction would give a frictional force opposite to that caused by the normal fluid viscosity and thus lower the rate of change of the surface slope. The effect of surface roughness in increasing the eddy viscosity has been studied recently by Fujii *et al.*[15] in a torsional oscillator.

At high heat currents in region $C$, because a curvature of the liquid surface focuses the light beam, we observe concave depressions in the liquid surface streaming from the heater with a swirling motion at about the normal fluid velocity of about of 1 cm/sec. These depressions result from vortices of macroscopic turbulence. At even higher power near $D$, large turbulent surface irregularities are observed, forming at the heater strip and moving outward. On gradually lowering the heater power to below where these irregularities first formed, a large surface discontinuity with a straight front parallel to the heater strip was observed to travel outward to the boundaries at a rate of about 1 cm/sec. This discontinuity as the heat current was lowered below the $C$ region apparently corresponds to the stationary front at higher heat currents as observed by Murphy, Castiglione, and Tough[11] in divergent channels. The discontinuity seems to mark a sudden change in liquid thickness between a state of aligned vorticity of the superfluid and a state of more nearly isotropic turbulence.

## CONCLUSIONS

This research has described some of the optical observation techniques that were used in studying turbulence and flow phenomena in thermal counterflow of $^4$He near 1 K. The techniques should be useful at much lower temperatures in order to avoid the pressure and heat transfer effects of the vapor. The method could be applied to high velocity superfluid flow without heat transfer by using superfluid filters. The analysis of heat flow in a thin layer of liquid helium with a free surface may be useful in analyzing results of optical studies of superfluid $^3$He-$B$ similar to those pioneered by the Helsinki group.[1] The present availability of lasers to observe the liquid surface contour greatly increases the accuracy and simplicity of the method. Optical fibers allow illumination with very little heat and the video camera can record transient effects. These advances could make optical observation an important method of studying the hydrodynamics of superfluids.

[1]A. J. Manninen, J. P. Pekola, G. M. Kira, J. P. Ruutu, A. V. Babkin, H. Alles, and O. V. Lounasmaa, Phys. Rev. Lett. **69**, 2392 (1992); J. P. O. Ruutu, H. Alles, A. V. Babkin, G. M. Kira, A. J. Manninen, J. P. Pekola, and O. V. Lounasmaa, Physica B **194-196**, 757 (1994).

[2]D. V. Osborne, Proc. R. Soc. London A **63**, 909 (1950).

[3]R. J. Donnelly, G. V. Chester, R. H. Walmsley, and C. T. Lane, Phys. Rev. **102**, 3 (1956); R. J. Donnelly, Phys. Rev. **109**, 1462 (1958).

[4]R. Meservey, Phys. Rev. **133**, A1471 (1964).

[5]A. V. Hershey, Phys. Rev. **56**, 204 (1939). The Hershey effect gives a height difference $\Delta h = [3(d\sigma/dT)/2\rho g h]\Delta T$ in this geometry, where $\sigma$ is the surface tension of $^4$He and the liquid depth $h \simeq 0.01$ cm. At 2.2 K, $\Delta h \approx 0.2$ cm/K and the absolute value decreases at lower temperatures. The thermomechanical effect $\Delta h = (S/g)\Delta T$, where $S$ is the entropy/unit mass, gives $\Delta h \approx 310$ cm/K at 1.1 K and $\Delta h \approx 9500$ cm/K at 2.0 K. Therefore, the Hershey effect is completely negligible in the superfluid region.

[6]L. D. Landau and E. M. Lifshitz, *Fluid Mechanics* (Pergamon, London, 1959), p. 236.

[7]L. D. Landau, J. Phys. (USSR) **5**, 71 (1941); L. D. Landau and E. M. Lifshitz, *Fluid Mechanics* (Ref. 6), p. 510.

[8]R. K. Childers and J. T. Tough, Phys. Rev. B **13**, 1040 (1976).

[9]J. T. Tough, in *Progress in Low Temperature Physics,* edited by D. F. Brewer (North-Holland, Amsterdam, 1982), Vol. 8.

[10]C. J. Gorter and J. H. Mellink, Physica **15**, 285 (1949).

[11]P. J. Murphy, J. Castiglione, and J. T. Tough, J. Low Temp. Phys. **92**, 307 (1993).

[12]K. W. Schwartz, Phys. Rev. B **38**, 2398 (1983).

[13]C. F. Barenghi, K. Park, and R. J. Donnelly, Phys. Lett. **84A**, 435 (1981).

[14]C. J. Swanson, Y. B. You, and R. J. Donnelly, Physica B **194-196**, 495 (1994).

[15]Y. Fujii, T. Ogawa, T. Shigematsu, M. Nakamura, M. Yamaguchi, and T. Shigi, Physica B **194-196**, 563 (1994).